SCIENTIFIC REPORTS

OPEN

Improved recovery time and sensitivity to H_2 and NH_3 at room temperature with SnO_x vertical nanopillars on ITO

Received: 24 March 2017
Accepted: 18 June 2018
Published online: 03 July 2018

L. D'Arsié[1,2], V. Alijani[1], S. T. Suran Brunelli[1], F. Rigoni[3], G. Di Santo[1], M. Caputo[1], M. Panighel[1,4], S. Freddi[3], L. Sangaletti[3] & A. Goldoni[1]

Nanostructured SnO_2 is a promising material for the scalable production of portable gas sensors. To fully exploit their potential, these gas sensors need a faster recovery rate and higher sensitivity at room temperature than the current state of the art. Here we demonstrate a chemiresistive gas sensor based on vertical SnO_x nanopillars, capable of sensing <5 ppm of H_2 at room temperature and 10 ppt at 230 °C. We test the sample both in vacuum and in air and observe an exceptional improvement in the performance compared to commercially available gas sensors. In particular, the recovery time for sensing NH_3 at room temperature is more than one order of magnitude faster than a commercial SnO_2 sensor. The sensor shows an unique combination of high sensitivity and fast recovery time, matching the requirements on materials expected to foster widespread use of portable and affordable gas sensors.

Gas sensors are indispensable in a modern society. Sensing H_2, for instance, is increasingly important, as this molecule is envisaged as an alternative to fossil energy sources[1]. For a safe transport and storage of H_2 to be viable, safety needs to be guaranteed, and therefore appropriate sensing for leakages[1]. In environmental monitoring, it is key to measure trace amounts also of other gases, such as CO, NO_2 and NH_3[2,3]. Indoors it is desirable to use simple and inexpensive sensors for detecting NO_2 and CO_2[3,4], to monitor air quality. Moreover, gas sensors can find applications in exams of medical conditions, for example through breath tests[5], as well as helping food quality control or contamination detection[6]. These are some of the many important applications of gas sensing, which explain the intense research in the field.

Today nanoscience allows the development of metal oxide sensing materials, promising dramatic changes in design and capabilities[7]. These improvements include the possibility to drastically reduce the size, weight, and power consumption, while increasing sensitivity and selectivity[8,9]. The widespread use of chemiresistive sensors is favoured by the ease of manufacturing requirements and low cost[10–13], in spite of a poor selectivity[14]. Chemiresistive sensors are therefore commercially very attractive, opposed to electrochemical sensors, which are unpopular for their short lifetime, and optical sensors, which are generally more expensive and bulky. A chemiresistive gas sensor consists of a sensitive material capable of changing its electrical properties when molecules of a certain gas are adsorbed on its surface. Tin dioxide (SnO_2), a wide band-gap semiconductor with remarkable chemical stability and electrical properties, is the most studied among semiconducting metal oxides for gas sensing applications[15,16]. Even if the selectivity is generally low, SnO_2 has demonstrated impressive sensitivity for a large range of types of gas. There is therefore strong interests in developing strategies aimed at enhancing the SnO_2-based device performance and selectivity. These include modifying the material morphology at the micro- and nano-scale, the bulk chemical composistion (i.e. doping), and by engineering the surface[17–21]. For instance, nanoparticles, nanowires, nanotubes and other nanoscale morphologies have enhanced gas-sensing properties[22,23], as a high surface area-to-volume ratio is key for enhancing the response due to the adsorption of

[1]Elettra – Sincrotrone Trieste S.C.p.A., s.s. 14 km 163.5 in Area Science Park, 34149, Trieste, Italy. [2]Department of Engineering, University of Cambridge, Cambridge, CB3 0FA, United Kingdom. [3]Interdisciplinary Laboratory for Advanced Materials Physics and Dipartimento di Matematica e Fisica, Università Cattolica del Sacro Cuore, Brescia, Italy. [4]Università degli Studi di Trieste, Piazzale Europa 1, 34127, Trieste, Italy. Correspondence and requests for materials should be addressed to L.D. (email: lorenzo.darsie@cantab.net) or A.G. (email: andrea.goldoni@elettra.eu)

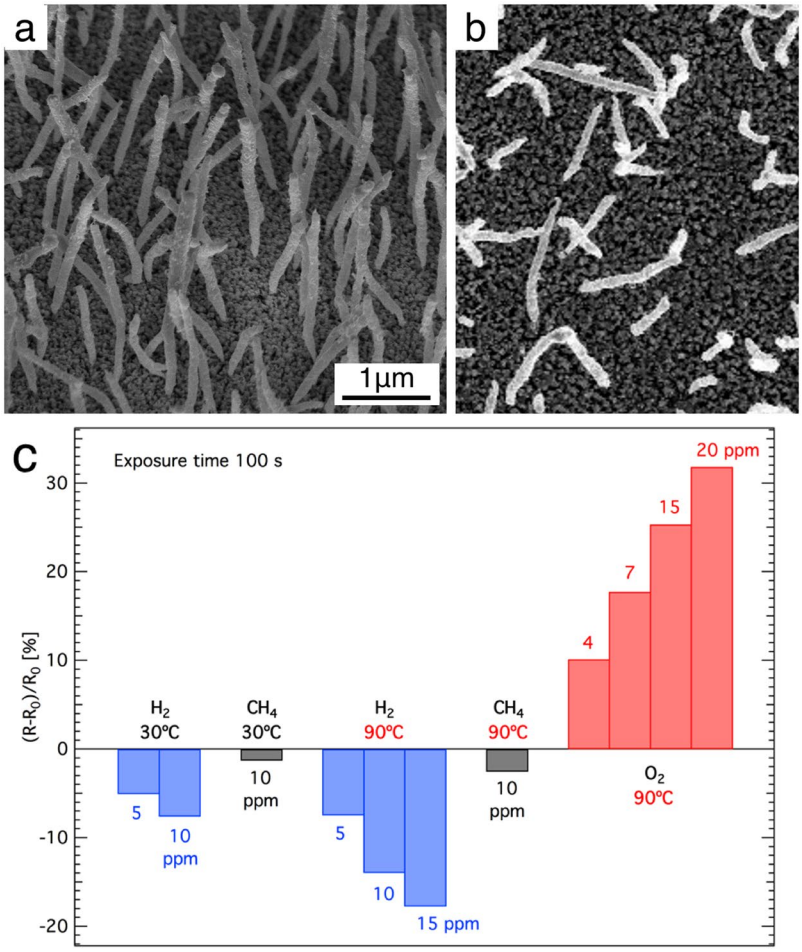

Figure 1. Scanning electron microscope images of vertical nanostructured SnO_x pillars on ~150 nm thick ITO Sn-reduced substrate. (**a**) 45° tilt angle, and (**b**) 0° tilt angle. The two figures share the same scale bar. The images are taken before starting the sensing tests and is representative of the post-sensing morphology, as no change can be noticed under the SEM. (**c**) Response of vertical nanostructured SnO_x pillars after exposure for 100 s to several gases at low temperatures (30 or 90 °C) in low vacuum (10^{-5} mbar).

molecules. Moreover, SnO_x chemiresistive sensors, when compared to competing sensing materials and techniques, are generally less expensive, lighter, more robust, and more sensitive to a wider range of gasses with quicker sensing and recovery times.

In order to fully develop SnO_x sensors, two main targets should be reached, namely short recovery time and sensitivity in the ppb range. Short recovery time is needed in situations of rapid modifications of gas concentrations. Whereas high sensitivity is necessary in applications that require the detection of low concentration gases (down to the ppt range), for instance in biochemical processes occurring in the human body and detected by analysing the breath of patients[5]. SnO_2 chemiresistors typically work in the temperature range 200–400 °C with a sensitivity that depends on the analyte gas, between 30 ppb and 500 ppm[15,24]. The recovery time is in the order of tens of seconds at high-temperature and often increases to several minutes at room temperature (RT). Elevated working temperatures are deleterious for energy consumption and therefore portability, as well as for safety during explosive gas detection, making efficient gas sensing at RT a highly desirable target.

Here we demonstrate that a chemiresistor based on vertical SnO_x nanopillars grown on Sn-reduced indium tin oxide (ITO) thin films[25] can detect 1 ppm of NH_3 at RT in air, with a recovery time of seconds, i.e. about an order of magnitude faster than commercially available metal oxide chemiresistor operating in the same conditions. It also detects few ppm of H_2 at RT in vacuum and, at high-temperature, it can recognize the equivalent of 10 ppt of H_2 (10^{-8} mbar). Thanks to the ease of fabrication and the efficient gas sensing characteristics, the proposed nanostructured material paves the way towards economic, safe, and portable gas sensors.

Results and Discussion

The vertical SnO_x nanopillars grown on ITO are shown in Fig. 1a,b. These sensing layers display huge resistivity variations for several gasses, already after an exposure in the ppm range for 100 s at RT. Figure 1c illustrates the variation in resistance $(R - R_0)/R_0$ [%] of the sensor to H_2, CH_4, and O_2 at RT and at 90 °C, where R is the resistance after 100 s of gas exposure and R_0 is the initial resistance before the introduction of gas in the experimental chamber. The experiment is performed in low vacuum (10^{-5} mbar as base-pressure). At 90 °C and 10 ppm, we

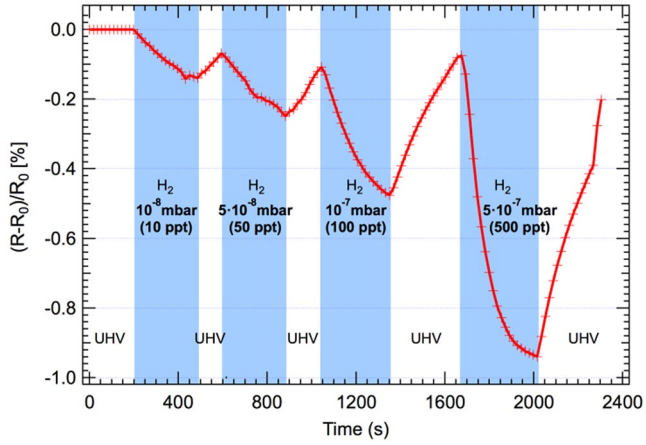

Figure 2. Response of SnO_x nanopillars sensor to low pressures of H_2 (corresponding to ppt amount) at 230 °C in UHV.

have observed resistivity variations in the range 15–20% for H_2 and O_2, while for CH_4 the sensitivity is one order of magnitude lower. These percentage changes are related to the relatively high initial resistance (R_0), which is of the order of 500 kΩ/sq. The sensor is insensitive to CO_2 and N_2 concentrations up to 1000 ppm. Moreover, similar treated substrates with nanometer roughness, i.e. ITO annealed at 670 ± 10 °C without any nanopillars, do no show sensitivity below 1000 ppm to all the analyte gases above indicated (see Supporting Information).

The observed behaviour can be explained by the effect of the gas molecules interacting with the n-type SnO_x nanopillars[26,27]. Negative charges trapped by oxidizing species generally cause an upward band bending, while the reaction with reducing gases, such as H_2, a downwards band bending. However, it is useful to notice that competitive adsorption and replacement of the adsorbed molecules could decrease or even reverse the band bending, resulting in an opposite variation in the conductivity[26,27].

It is important to remark that the ITO layer does not contribute appreciably to gas sensing, as discussed in the SI (Figs SI.1 and SI.2). In fact attempts to use an ITO layer without nanopillars as a sensor yielded only a variation of the order of 0.2–0.5% after the introduction of 1000 ppm of H_2, CH_4, O_2, N_2, CO_2 per 100 s at RT.

To further investigate the sensitivity to H_2 at high temperature, we place the sample at 230 °C in ultra-high-vacuum (UHV, 10^{-10} mbar) chamber. This allows us to expose the sensor to small amounts of gas (10^{-8}). Although UHV experiments do not replicate sensor typical operational conditions, in very low-pressure experiments it is possible to analyse the sensor with a higher signal-to-noise ratio and precision. At the same time, the preparation and characterization of the sample in UHV appears to be an important step to identify and properly address the chemo-physical processes that occur at the surface of the sensor.

The resistivity of the sample increases to about 3 MΩ in UHV after removing all carbon contamination by annealing at 300 °C in an oxygen atmosphere (10^{-7} mbar). Figure 2 shows the response of the SnO_x nanopillars from 10^{-8} mbar up to 5×10^{-7} mbar (ppt amounts) of H_2, expressed as $(R - R_0)/R_0$ [%]. It can be observed that the chemiresistor is sensistive at least to 10^{-8} mbar (10 ppt) of H_2.

It is worth noting that at these concentrations and at 230 °C the sensor does not respond to CH_4, CO_2, CO, NO_2 and N_2. The X-ray photoemission data of Sn 3d peaks collected during the 5×10^{-7} mbar of H_2 exposure are reported in the Supporting Information (Fig. SI.3). The Sn 3d peaks show a shift to higher binding energy when the gas is introduced and revert back to the initial binding energy when the gas is removed and the chamber reaches the base pressure of 10^{-10} mbar, in agreement with the expected variation of the band bending. This recovery to the initial conditions observed through XPS core level analysis further confirms the reversible character of the interaction of the target molecules with the chemiresistor.

In order to further investigate the response and the recovery time of our chemiresistive sensor, we have compared it to a commercial sensor for NH_3 (FIGARO TGS 2602). Our sample is operated at RT, while the FIGARO requires heating at 200 °C. The same measurements performed on 4 sensors show reproducibility across different substrates, as shown in the SI (Fig. SI.4). Our sensor follows the FIGARO response, but presents more oscillations, see Fig. 3. A comparison of fluctuations and noise amplitude in of Fig. 3b,c, respectively, should suggest that this behaviour is not a read-out noise amplitude fluctuation. It can be attributed to local partial pressure variations of the order of 1 ppm or less while exposing the sensor to 30 ppm of NH_3 from a point-like source in ambient air. This is confirmed in Fig. 3d where for exposures to a lower ammonia concentration (3.6 and 2.2 ppm), as well as for a reduced time, the fluctuations are greatly reduced. The presence of these fluctuations, however, is not related to the response time (which is very short for both SnO_x and FIGARO), but to the very rapid recovery time with respect to the FIGARO behaviour. As shown in Fig. 3, when the NH_3 is pumped away, the overall recovery of our sensor is so fast that in less than 200 s the initial resistance is completely recovered, while the reference FIGARO sensor has not yet fully recovered. It is also worth noting that the recovery does not follow a simple exponential behaviour, as the process takes place with two different time scales. We therefore fit this behaviour using a decreasing double exponential function with exponential constants τ_1 and τ_2. The obtained recovery time gives a τ_1 value of few seconds (3.5 s in Fig. 3a and 2.7 s in Fig. 3d) and τ_2 of tens of seconds, both of which are about one

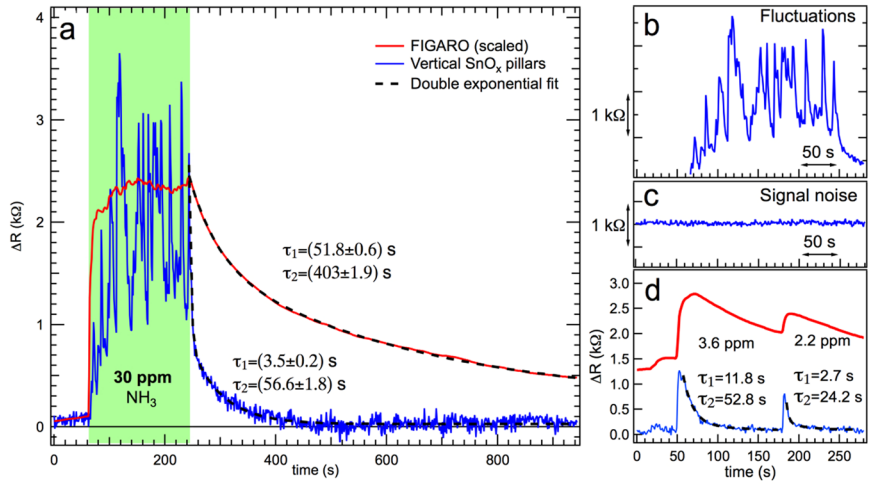

Figure 3. (**a**) Resistivity variation of the vertical SnO_x nanopillars sensor (blue line) compared with the FIGARO sensor (dashed red line) after an exposure to 30 ppm of NH_3 in air at RT. The NH_3 exposure period has been marked with a green background. Both recovery times are fitted with double exponential functions, illustrated by dashed black lines. (**b**) Observed fluctuations can be compared with (**c**) the signal noise. (**d**) Shows the resistivity variation of our vertical SnO_x nanopillars sensors (blue line) compared with the FIGARO response (dashed red line) after an exposure to 3.6 and 2.2 ppm of NH_3 (pulse in the millisecond range).

order of magnitude lower than the same fitting procedure for the recovery time of FIGARO sensor. The presence of τ_1 and τ_2 in both sensors may be related to different interactions of the physisorbed NH_3 molecules with the substrate.

The difference in recovery rates shown in Figs 2 and 3 can be attributed to the inefficient H_2 pumping by turbo-molecular pumps and the large volume of the experimental chamber. The resistance recovery rates in Fig. 2 are a convolution of the sensor recovery and the slow pressure recovery rates. The sensing test with H_2 in ambient air could not be performed for health and safety regulations.

In addition to fast response, also selectivity and stability are important characteristic of gas sensing. Selectivity in air has been checked by exposing the sensor to different gasses. As detailed in the SI (Fig. SI.5), sensor is not sensitive to acetone, 2-propanol, and sodium hypochlorite. Response to ethyl alcohol is quite low as compared to ammonia.

Furthermore the response to ammonia was tracked for long exposure times (250–300 seconds) and high concentrations (50–70 ppm). In spite of the prolonged interaction with large concentration of gas, full recovery was attained due to the fast recovery time (Fig. SI.6). Response to humidity was also investigated and the sensor displayed a resistance drop with humidity increase (Fig. SI.7), consistently with an n-type behaviour.

Finally, stability in ambient air for relatively long periods (24 hours) has been checked several times during our experiments. As shown in the supplementary information (Fig. SI.8), the sensors were quite stable with a base resistance that did not change across the time, unless the outer conditions (temperature or relative humidity) changed along the monitoring time.

The very fast recovery rate of our sensor is outstanding when compared with results in literature. However, other promptly responsive RT sensors have been reported[28–32]. Favier *et al.*[30], for instance, have produced Pd nanowires sensors with a 90% signal saturation reached in less than 80 ms at RT. These fast responses are however achieved with very high H_2 concentrations (20–100 ppm). They propose a sensing mechanism that involves the closing of nanoscopic gaps or "break junctions" caused by the dilation of wire grains. This creates a sensor that works more as an on/off switch than a continuous detection, which explains the excellent results at high concentrations, but also a high gas detection threshold (5–10 ppm). Changing the geometry of the Pd nanostructures can enhance the sensitivity to lower detection limits, although penalising recovery rates[31].

Finally, our sensor can detect at least 1 ppm of NH_3 at RT (see Fig. 4), which is comparable with recent results in literature, in which however, the sensing response/recovery rates are high. Mubeen *et al.*[33] for instance, reported the detection of 0.5 ppm of NH_3 at RT, using single wall carbon nanotubes decorated with tin oxide, but the response/recovery rates are in the time scale of several minutes.

The interaction of target gas molecules with the oxide nanopillars follows the reaction channels widely discussed in literature for oxide materials (see SI, Eq. 1–4 and references S1–S10). The adsorption mechanism can in principle also depend on the environment where exposure to target molecules occurs. As the present sensors have been tested under different conditions (ultra-high vacuum, low vacuum - hereafter denoted as "vacuum" - and ambient air), it is worth discussing the observed behaviour at the light of the different working atmospheres. The main difference between the two environments (ambient air and vacuum) is the presence of oxygen. In air, O_2 quickly adsorbs on the surface and provides a key feature for the interaction with target molecules. It is important to observe that upon exposure to ammonia in ambient air the sensing layer behaves as a p-type system (i.e. resistivity increases upon exposure to a reducing molecule, Fig. 3). In turn, in vacuum conditions a resistivity increase for oxidizing target molecules (O_2) is observed, and a resistivity decrease is observed upon exposure to

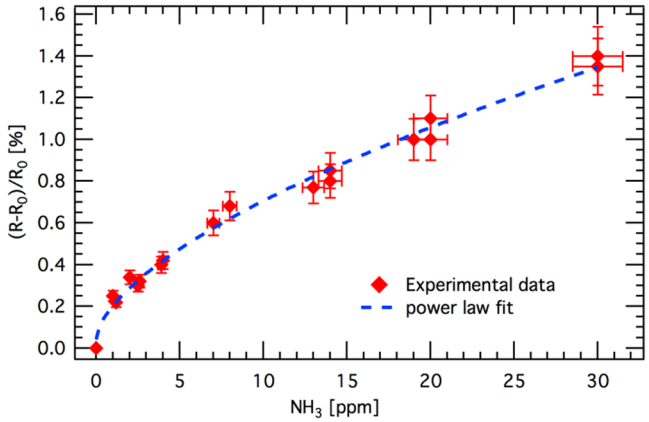

Figure 4. Experimental response of the sensor as a function of NH_3 exposure at RT in air, with about 50% of relative humidity. The power law fit is meant as a guide for the eye.

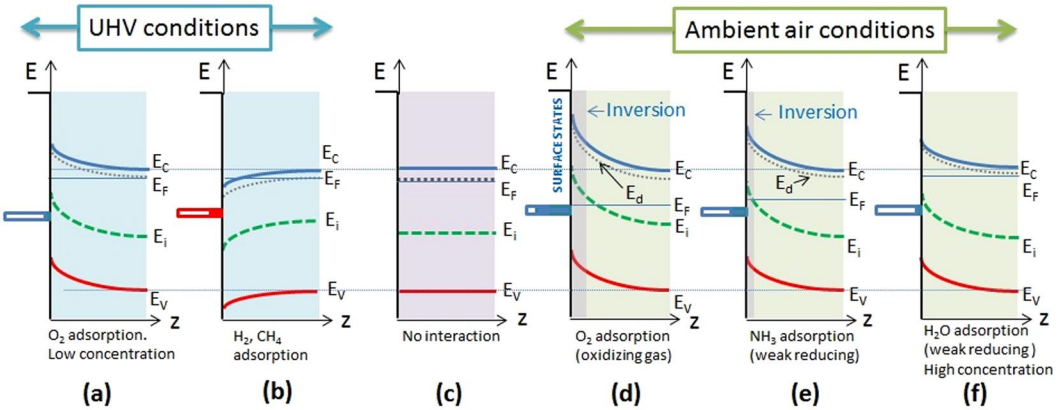

Figure 5. Schematic diagrams of the nanopillar electron bands under different conditions (UHV and ambient air) after exposure to different gases. (**a**) O_2 in UHV, (**b**) H_2 or CH_4 in UHV, (**d**) O_2 in air, (**e**) NH_3 in air with pre-adsorbed O_2, (**f**) H_2O in air with pre-adsorbed O_2. (**c**) Reference band diagram for the n-doped SnO_x nanopillars. The dotted lines represent the donor level (E_d), the dashed line the intrinsic Fermi level (E_i).

reducing molecules (CH_4, H_2, Fig. 1c). In this case the sensing layer behaves as an n-type semiconductor. The result obtained in vacuum conditions is expected, as both SnO_2 and ITO are classified among n-type semiconductor oxide materials. The behaviour in air upon exposure to ammonia can be explained on the basis of the scheme proposed by Oprea *et al.*[34]. The authors suggest that an n-type semiconductor can display a p-type inversion layer upon O_2 adsorption and therefore a weakly reducing gas can increase the inversion layer resistivity, as far as the inversion condition is maintained. Consistently with this finding, we observe that humidity has the opposite effect, i.e. humidity increase determines a resistivity drop. In this case, the concentration of water molecules is much higher than the NH_3 case and the effect of reducing molecules could quench the inversion layer and restore the n-type behavior. The different testing conditions are depicted in Fig. 5.

Once band bending effects and the dual (n-type o p-type) operating condition has been elucidated, one is left with the effects of morphology and transport through the junctions.

Chemical sensing is about surface and interface interactions between the analyte molecules and the sensing material. Nanostructured sensors, for example made of nanotubes, nanowires or nanoclusters of SnO_2, exhibit a high surface area-to-volume ratio, which strongly improves gas detection. The mechanism envisioned involves the adsorption, diffusion, electron transfer, as well as the change in the depletion zone related to the analyte molecule at the nanowire/surface junctions. In nanostructured materials, the sensitivity is usually related to the highly resistive nodes formed at the interfaces between different nanostructures. This was well demonstrated by Kolmakov *et al.*[35] using photoemission microscopy on SnO_2 nanowires between two metallic electrodes. They analyse the properties of individual SnO_2 nanowires in a network of active elements in chemiresistor devices, showing the *in-situ* characterization of electron transport properties of mats of percolating nanostructures. It was shown that the transport quality depends on the interfaces between the nanowires. Therefore, reducing the number of interface junctions between the nanostructures as much as possible before reaching the electrodes is a likely way to increase the detection limit of the chemiresistor sensor. In our sample, the SnO_x nanostructures are vertical (see Fig. 1a), typically isolated, with the only interface being the one with the ITO Sn-reduced substrate. Since the

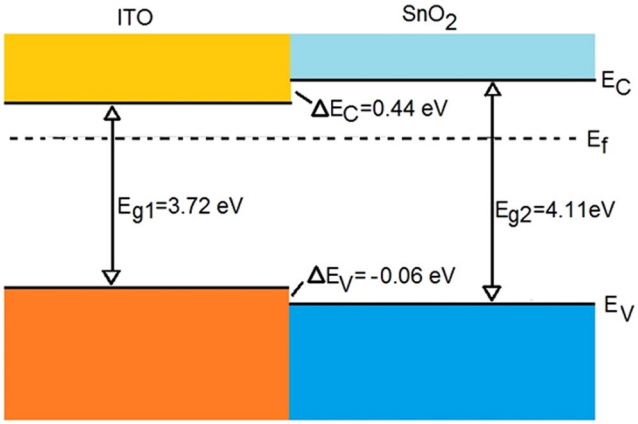

Figure 6. Energy band alignment at the ITO/SnO_2 isotype heterojunction (adapted from ref.[37]).

nanopillars don't touch each other enough to make a continuous path between the electrodes, the current flows in the Sn-depleted ITO film only. We thereby completely remove all resistive nodes between the nanopillars keeping only the interfaces with the substrate. We are therefore benefitting from the high surface area of the nanostructured SnO_2, without the need of any deleterious resistive nodes in the resistive channel.

In the present case, high sensitivity is obtained by combining the surface reactivity with an efficient transport of charges from the nanopillars to the substrate. Molecules interact with the surface layer and charge flows through this layer to the substrate. The sensor quickly tracks the concentration variation and the response can be assumed to scale with concentration according to the calibration curve, providing high sensitivity. On the other hand, a fast recovery allows to quickly resumes the initial R_0 conditions, avoiding bias in the response due to a long recovery time. The response time is estimated as the time occurring for the signal to rise from 10% to 90% of the overall signal change (ΔR). In our system the signal sampling is carried out with a frequency of $1/1.16\,s^{-1}$. Therefore the response time measure is actually limited by the read-out frequency. Faster times may occur, but they are not detectable.

The sensor resistance depends on possible potential barriers and on the number of conducting charges present in the large surface area of vertical nanopillars due to the analyte gas[36]. So, the mechanism that determines a greater response to the gases is twofold, involving both the morphology and the electronic properties (i.e. band alignment) of the heterojunctions established in the sensing layer.

(I) Morphology. The lack of contact points between the pillars excludes of percolation type mechanisms and therefore makes more efficient transport of the charges. This implies that the only interface involving the nanopillars is the interface between each single nanopillar and the ITO substrate. Sensing elements are well separated from each other allowing for chemisorption and fast desorption without trapping between pillars or inter-grain trapping as in polycrystalline thick and thin films. In these conditions, transport ultimately occurs across a single junction (SnO_2-ITO) rather than being an inter-grain tunneling. This leads to efficient charge collection.

(II) Heterojunction. The interface above mentioned can be modelled as an heterojunction (HJ) between a SnO_x nanopillar and the ITO substrate (that contributes as an electrode to collect charge from the pillars). Assuming that close to the junction both systems are n-type materials, the heterojunction can be classified as an isotype junction and the band offset diagram for this type of system (ITO/SnO_2) is discussed in ref.[37]. The energy band diagram, adapted from Tingliang *et al.*[37], is shown in Fig. 6.

According to this diagram, a charge injection/extraction on the SnO_2 side would end up in the ITO layer due to the favourable energy level mismatch both for holes and electrons. Indeed, the diagram presents a band alignment typical of a type I (i.e. straddling) HJ, where the material displaying a larger gap is SnO_2 (4.11 eV), while the energy gap of ITO is 3.72 eV. With this type of junction, charges injected to the SnO_x sensing "layer" flow towards the substrate ITO because the minimum of the conduction band of SnO_x is above the minimum of the conduction band of the ITO. The same holds for holes injected in the SnO_x layer. They would flow to the ITO side as the ITO VB maximum is above the VB maximum of SnO_2.

Room temperature operation is becoming an important topic in the field of gas sensing, as reported by a recent review[38]. According to the authors, 1D semiconductor nanostructures such as nanowires, nanofibers, and nanotubes can demonstrate appealing room-temperature sensing performances. Among metal oxides, In_2O_3-based nanostructures (i.e. nanowires and nanotubes) were found to operate at room temperature with a good sensitivity towards ammonia[39], NO[40], and H_2S[41], Likewise, also SnO_2 nanostructures has shown remarkable RT sensitivity towards ethanol, CO, H_2, and NO_x[17,42]. In spite of these results, the mechanisms underlying RT operation still needs to be properly assessed.

The characteristic mechanism of metal oxide based sensors operating at high temperature is usually termed as combustive gas sensing effect, in which adsorbed analyte molecules become oxidised by interactions with pre-adsorbed surface oxygen ions[43]. In fact, those chemical surface interactions that lead to a combustive gas response are thermally activated. Thermal activation is not expected at low temperatures, and therefore evidence of significant low temperature sensing must have a different origin.

A discussion on alternative mechanism can be found in ref.[44], where authors present sensors based on $W_{18}O_{49}$ nanowires with remarkable room-temperature sensitivity to NO_2. The sensitivity is shown to decrease with

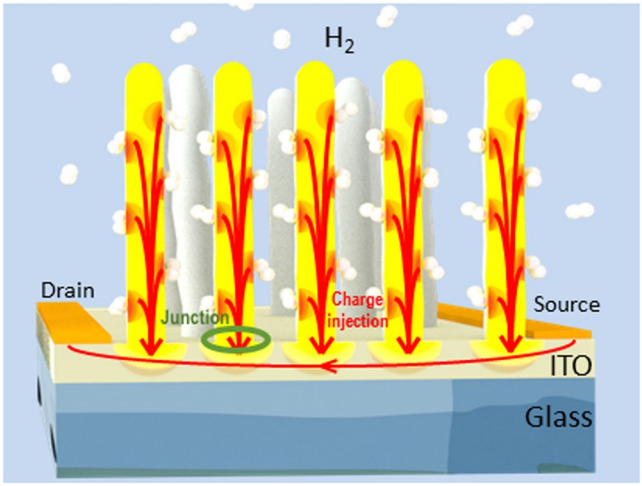

Figure 7. Schematic of the electron injection from the SnO_2 nanopillars to the substrate upon the exposure to a reducing gas. The only junctions are at the nanopillar/ITO interface. Therefore, the current from source to drain does not have to pass through any junction.

temperature, rather than being higher, as usually found in metal oxide nanoparticles. The intensity of the sensor signals decreases drastically with temperature, up to being unresponsive to NO_2 above 300 °C. The experimental results were found to be consistent with the model developed by Gurlo *et al.*[45], thus indicating the formation of surface-trapped states NO_2, including no evidence of dissociative NO_2 adsorption. For the case of the present SnO_x nanorods, it is likely that the same mechanisms are at work, leading to a remarkable response at room temperature.

In addition to room temperature operation, several studies reported fast recovery in oxide nanofibers or, in general, in 1D nanostructures[46–48].

In spite of the many studies, the mechanisms of fast recovery have not yet been assessed. However a common feature is represented by the unique, nearly 1D, structure of all these nanostructured oxides. Indeed, these systems usually display large specific surface areas, which may result in the absorption of large amounts of gas molecules. Charge accumulation layers are formed as oxygen molecules absorb to the surface of the materials. These accumulation layers may overlap with each other along the rod/fiber/pillar direction, producing continuous charge transfer channels. Charge mobility along this channels, together with a relatively low adsorption energy which favours molecules detachment, can be regarded as the mechanisms underlying the fast recovery. In other words, the fast recovery is determined by the capability to quickly drain the charge along the charge transfer channels before the weakly bound target molecules detach from the surface.

Figure 7 schematically shows the overall charge flow in the sensor, from charge injection at the nanopillars surface down to the ITO sensing layer. A similar behavior was observed by Pan *et al.*[49], which describe the effect as one-dimensional nanostructures gating the conducting channel in a two-dimensional ZnO nanocomb.

Conclusions

We have reported a molecular architecture of SnO_x sensors that allows a detection of H_2 below 5 ppm at RT and to a partial pressure of 10^{-8} mbar (10 ppt) at 230 °C. Using NH_3 in air we observe a recovery time that is more than one order of magnitude faster than a commercial SnO_2 sensor and faster than any other sensor detecting low concentrations (1 ppm) reported in literature. The combination of high sensitivity and fast recovery rates are explained by the unique nanostructuring of ITO in our device, which presents tin oxide vertical nanopillars on Sn-depleted ITO high-resistive layer.

The response to target molecules can be strongly determined by different environments (vacuum *vs* air). In vacuum the sensors behaves as n-type oxide semiconductor. Adsorption of O_2 in air is likely to yield an inversion layer, which turns an n-type response into a p-type response of the SnO_x pillars. Charge transport occurs along the pillars surface until the SnO_x-ITO interface is encountered. Here, charge transfer to the ITO layers occurs due to the favourable band alignment for both n-type and p-type carriers. We suggest that the remarkable sensitivity and the response rates of our system will enable portability for a wide range of applications.

Methods

Sample preparation. The sample is prepared starting from a ITO/glass substrate exposed sequentially to H_2 and C_2H_2 at ~650 °C. This process forms vertical nanostructures of carbon filled with tin, as previously reported in detail[25]. The carbon shell can then be burned by heating the sample in oxygen at ~650 °C. Note that no further change to the structures are observed at this temperature, once the carbon is burned away. The final sensor is therefore made of a glass supports, coated with a Sn-depleted ITO film, ~120 nm thick, covered with vertical nanopillars of SnO_x, see Fig. 1a,b. Ag metal electrodes are painted at both ends of the Sn-reduced ITO substrate.

Gas sensing tests. The H_2 measurements shown in Figs 1 and 2 are performed at the μ- & nano-carbon laboratory and SuperESCA beamline of the Elettra synchrotron in Trieste, where electrical measurements and X-ray photoemission spectra can be acquired in parallel. The base pressure in the chamber is ~10^{10} mbar and the dosed gas is measured with a hot filament pressure gauge. The chamber is pumped with turbo-molecular pumps.

The NH_3 sensing measurements shown in Figs 3 and 4 are performed at I-Lamp laboratory in Brescia, the gas concentration is measured with a calibrated FIGARO TGS 2602 sensor. Both our and the Figaro sensors, are mounted on a specifically designed circuit exposing the sensors to a point-like source of NH_3. In the same setup, humidity and temperature sensors are also mounted. Further details can be found in refs[50,51].

References

1. Dutta, S. A review on production, storage of hydrogen and its utilization as an energy resource. *J. Ind. Eng. Chem.* **20**, 1148–1156 (2014).
2. Andio, M. Sensor Array Devices Utilizing Nano-structured Metal-oxides for Hazardous Gas Detection, *Ph.D thesis*, The Ohio State University (2012).
3. Huang, L. *et al*. Fully printed, rapid-response sensors based on chemically modified graphene for detecting NO_2 at room temperature. *ACS Appl. Mater. Interfaces* **6**, 7426–7433 (2014).
4. Trung, D. *et al*. Selective detection of carbon dioxide using LaOCl-functionalized SnO_2 nanowires for air-quality monitoring. *Talanta* **88**, 152–159 (2012).
5. Righettoni, M., Amann, A. & Pratsinis, S. Breath analysis by nanostructured metal oxides as chemo-resistive gas sensors. *Mater. Today* **18**, 163–171 (2015).
6. Baldwin, E., Bai, J., Plotto, A. & Dea, S. Electronic Noses and Tongues: Applications for the Food and Pharmaceutical Industries. *Sensors* **11**, 4744–4766 (2011).
7. Sharma, S. & Madou, M. A new approach to gas sensing with nanotechnology. *Phil. Trans. R. Soc. A* **370**, 2448–2473 (2012).
8. Penner, R. Chemical Sensing with Nanowires. *Annu. Rev. Anal. Chem.* **5**, 461–485 (2012).
9. Kolmakov, A. & Moskovits, M. Chemical Sensing and Catalysis by One-Dimensional Metal-Oxide Nanostructures. *Annu. Rev. Mater. Res.* **34**, 151–180 (2004).
10. Vishinkin, R. & Haick, H. Nanoscale Sensor Technologies for Disease Detection via Volatolomics. *Small* **11**, 6142–6164 (2015).
11. Di Natale, C., Paolesse, R., Martinelli, E. & Capuano, R. Solid-state gas sensors for breath analysis: A review. *Analytica Chimica Acta* **824**, 1–17 (2014).
12. Montuschi, P., Mores, N., Trové, A., Mondino, C. & Barnes, P. J. The Electronic Nose in Respiratory Medicine. *Respiration* **85**, 72–84 (2013).
13. Ellis, J. E. & Star, A. Carbon Nanotube-based Gas Sensors toward Breath Analysis. *ChemPlusChem* **81**, 1248–65 (2016).
14. Smulko, J. *et al*. New approaches for improving selectivity and sensitivity of resistive gas sensors: a review. *Sensor Rev.* **35**, 340–347 (2015).
15. Miller, T., Bakrania, S., Perez, C. & Wooldridge M. Nanostructured Tin Dioxide Materials for Gas Sensor Applications, Chapter 30 in Functional Nanomaterials, Edited by Kurt E. Geckeler and Edward Rosenberg (2006).
16. Sberveglieri, G. *et al*. Synthesis and integration of tin oxide nanowires into an electronic nose. *Vacuum* **5**, 532–535 (2012).
17. Wang, Y., Jiang, X. & Xia, Y. A Solution-Phase, Precursor Route to Polycrystalline SnO_2 Nanowires That Can Be Used for Gas Sensing under Ambient Conditions. *J. Am. Chem. Soc.* **125**, 16176–16177 (2003).
18. Mädler, L. *et al*. Sensing low concentrations of CO using flame-spray-made Pt/SnO2 nanoparticles. *J. Nanopart. Res.* **8**, 783–796 (2006).
19. Wu, J. A room temperature ethanol sensor made from p-type Sb-doped SnO_2 nanowires. *Nanotechnology* **21**, 235501 (2010).
20. Hwang, I. *et al*. Facile control of C_2H_5OH sensing characteristics by decorating discrete Ag nanoclusters on SnO_2 nanowire networks. *ACS Appl. Mater. Interfaces* **3**, 3140–3145 (2011).
21. Li, X., Cho, J., Kurup, P. & Gu, Z. Novel sensor array based on doped tin oxide nanowires for organic vapor detection. *Sens. Actuators B–Chem.* **162**, 251–258 (2012).
22. Comini, E. & Sberveglieri, G. Metal oxide nanowires as chemical sensors. *Mater. Today* **13**, 36–44 (2010).
23. Carpenter M., Mathur S. & Kolmakov A. (eds) Metal Oxide Nanomaterials for Chemical Sensors, Springer, Heidelberg (2013).
24. Dattoli, E., Davydov, A. & Benkstein, K. Tin oxide nanowire sensor with integrated temperature and gate control for multi-gas recognition. *Nanoscale* **4**, 1760–1769 (2012).
25. D'Arsiè, L. *et al*. Tubular Sn-filled carbon nanostructures on ITO: Nanocomposite material for multiple applications. *Carbon* **65**, 13–19 (2013).
26. Sberveglieri, G. Gas Sensors. *Kluwer Academic Publishing*, Berlin, Germany (1992).
27. Leblanc, E. *et al*. NO_x adsorption onto dehydroxylated or hydroxylated tin dioxide surface. Application to SnO_2-based sensors. *Sens. Actuators B-Chem.* **62**, 67–72 (2000).
28. Li, H. *et al*. High-temperature humidity sensors based on WO_3–SnO_2 composite hollow nanospheres. *J. Mater. Chem. A* **2**, 6854–6862 (2014).
29. Pan, X., Zhao, X., Chen, J., Bermak, A. & Fan, Z. A fast-response/recovery ZnO hierarchical nanostructure based gas sensor with ultra-high room-temperature output response. *Sens. Actuators B-Chem.* **206**, 764–771 (2015).
30. Favier, F., Walter, E., Zach, M., Benter, T. & Penner, R. Hydrogen Sensors and Switches from Electrodeposited Palladium Mesowire Arrays. *Science* **293**, 2227–2231 (2001).
31. Im, Y. *et al*. Investigation of a Single Pd Nanowire for Use as a Hydrogen Sensor. *Small* **2**, 356–358 (2006).
32. Yang, S. *et al*. Highly Responsive Room-Temperature Hydrogen Sensing of α-MoO_3 Nanoribbon Membranes. *ACS Appl. Mater. Interfaces* **7**, 9247–9253 (2015).
33. Mubeen, S. *et al*. Hybrid tin oxide-SWNT nanostructures based gas sensor. *Electrochim. Acta* **92**, 484–490 (2013).
34. Oprea, A., Bârsan, N. & Weimar, U. Work function changes in gas sensitive materials: Fundamentals and applications. *Sensors and Actuators B* **142**, 470–493 (2003).
35. Kolmakov, A. *et al*. Spectromicroscopy for Addressing the Surface and Electron Transport Properties of Individual 1-D Nanostructures and Their Networks. *ACS Nano* **2**, 1993–2000 (2008).
36. Yamazoe, N. & Shimanoe, K. Theory of power laws for semiconductor gas sensors. *Sens. Actuators B-Chem.* **128**, 566–573 (2008).
37. Liu, T. *et al*. Interface Study of ITO/ZnO and ITO/SnO_2 Complex Transparent Conductive Layers and Their Effect on CdTe Solar Cells. *Int. J. Photoenergy*, Article ID 765938 (2013).
38. Zhang, J., Liu, X., Neri, G. & Pinna, N. Nanostructured Materials for Room-Temperature Gas Sensors. *Adv. Mater.* **28**, 795–831 (2016).
39. Du, N. *et al*. Porous Indium Oxide Nanotubes: Layer-by-Layer Assembly on Carbon-Nanotube Templates and Application for Room-Temperature NH_3 Gas Sensors. *Adv. Mater.* **19**, 1641 (2007).
40. Chinh, N. *et al*. NO gas sensing kinetics at room temperature under UV light irradiation of In_2O_3 nanostructures. *Sci. Rep.* **6**, 35066 (2016).

41. Xu, L. *et al*. Electrospinning preparation and room temperature gas sensing properties of porous In_2O_3 nanotubes and nanowires. *Sens. Actuators B* **147**, 531 (2010).
42. Jiang, C., Zhang, G., Wu, Y., Li, L. & Shi, K. Facile synthesis of SnO_2 nanocrystalline tubes by electrospinning and their fast response and high sensitivity to NO_x at room temperature. *CrystEngComm.* **14**, 2739 (2012).
43. Ahlers, S., Muller, G. & Doll, T. "Factors influencing the gas sensitivity of metal oxide materials," in Encyclopedia of Sensors, Grimes, C. A., Dickey, E. C. and Pisko, M. V., Eds., vol. 3, pp. 413–447, The Pennsylvania State University, University Park, Pa, USA, (2006).
44. Polleux, J. *et al*. Template-Free Synthesis and Assembly of Single Crystalline Tungsten Oxide Nanowires and their Gas-Sensing Properties. *Angew. Chem. Int. Ed.* **45**, 261–265 (2006).
45. Gurlo, A., Barsan, N., Ivanovskaya, M., Weimar, U. & Göpel, W. In_2O_3 and MoO_3–In_2O_3 thin film semiconductor sensors: interaction with NO_2 and O_3. *Sens. Actuators B* **47**, 92 (1988).
46. Fan, H., Xu, X., Ma, X. & Zhang, T. Preparation of $LaFeO_3$ nanofibers by electrospinning for gas sensors with fast response and recovery. *Nanotechnology* **22**, 115502 (2011).
47. Liang, Q. *et al*. Room-temperature NH_3 sensors with high sensitivity and short response/recovery times. *Chin. Sci. Bull.* **59**, 447 (2014).
48. McCormack, R. *et al*. Laser irradiated nano-architectured undoped tin oxide arrays: mechanism of ultrasensitive room temperature hydrogen sensing. *Nanoscale* **4**, 7256–7265 (2012).
49. Pan, X., Liu, X., Bermak, A. & Fan, Z. Self-Gating Effect Induced Large Performance Improvement of ZnO Nanocomb Gas Sensors. *ACS Nano* **10**, 9318–9324 (2013).
50. Chiesa, M. *et al*. Development of low-cost ammonia gas sensors and data analysis algorithms to implement a monitoring grid of urban environmental pollutants. *J. Environ. Monit.* **14**, 1565–1575 (2012).
51. Rigoni, F. *et al*. Enhancing the sensitivity of pristine carbon nanotubes to detect low-ppb ammonia concentrations in the environment. *Analyst* **138**, 7392 (2013).

Acknowledgements

We acknowledge Sabina Caneva for the 3D schematics and A. Kolmakov for discussions. V.A. acknowledges the Italian Ministero dell'Istruzione, dell'Universitá e della Ricerca (FIRB Nanosolar RBAP11C58Y_003) and A.G. thank the NATO – G51 project.

Author Contributions

L.D. grew the sensing samples; L.D. and A.G. performed and analysed the gas sensing measurements shown in Figure 1; V.A.Z., S.T.S.B., G.D.S., M.C., M.P. and A.G. performed and analysed the gas sensing measurement shown in Figure 2; F.R., S.F. and L.S. performed and analysed the gas sensing measurements shown in Figure 3 and Figure 4; All the authors collaborated to the other figures of the paper. L.D. and A.G. wrote the manuscript with the contribution of all the other authors.

Additional Information

Supplementary information accompanies this paper at https://doi.org/10.1038/s41598-018-28298-w.

Competing Interests: The authors declare no competing interests.

Publisher's note: Springer Nature remains neutral with regard to jurisdictional claims in published maps and institutional affiliations.